RESEARCH ARTICLE

Detection of lead ions using an electrochemical aptasensor

Mohsen Adabi

Department of Metallurgy and Materials Engineering, Faculty of Engineering, Roudehen Branch, Islamic Azad University, Roudehen, Iran

ARTICLE INFO

ABSTRACT

The aim of this work was to develop a simple, selective and sensitive aptasensor for detection of Pb^{2+} based on hairpin structure of complementary strand (CS) of aptamer (Apt). Screen printed carbon electrode (SPCE) was electrodeposited by gold nanoparticles to be used as the substrate for the immobilization of Apt-CS. Moreover, gold nanoparticles (AuNPs) and thionine were added to increase the sensitivity of the aptasensor. The morphology of SPCE and AuNPs modified SPCE was investigated using scanning electron microscopy (SEM). The SEM results exhibited that the AuNPs were homogeneously distributed on the surface of SPCE. The electrochemical performance of aptasensor was evaluated by means of cyclic voltammetry (CV) and differential pulse voltammetry (DPV) measurements. The electrochemical results indicated that peak current due to the hairpin structure formation of CS decreased in the presence of Pb^{2+}. However, in the absence of Pb^{2+}, peak current was enhanced because of combination of thionine/AuNPs-CS. The designed aptasensor showed a high selectivity toward Pb^{2+}, wide linear range (1-40 nM), low detection limit (374 pM), acceptable reproducibility and good long-term stability.

How to cite this article

INTRODUCTION

The detection and monitoring of lead ions in the environment due to extensive use of lead metal at different industrials such as a automotive, petroleum and paint has became a worldwide concern nowadays [1, 2]. Since lead ions (Pb^{2+}) are non-biodegradability, they can lead to detrimental effects on human health like neurological allergy, memory loss, muscle paralysis and anemia even at trace concentration [3]. According to the Center of Disease Control and Prevention, the maximum allowable concentration of Pb^{2+} in the blood is 10 μg dL^{-1} [4].

In view of the adverse effects of Pb^{2+} on human health, it needs to develop simple, precise, convenient, reliable and sensitive methods for the detection of this element in different environments [5]. The most common techniques for Pb^{2+} monitoring include colormetric, fluorescent and electrochemistry. Although these methods have

shown good performance in the determination of Pb^{2+}, they cannot carry out accurate analysis at trace levels [6, 7]. To overcome this problem, the electrochemical nano-biosensors due to their high sensitivity, cost effective, rapid response and easy data read-out have been developed [8-10].

Recently, the use of DNA for the detection of metal ions because of its good stability, high solubility in aqueous solution and high affinity binding toward some metal ions has been increased [11]. Aptamers mainly selected through the SELEX (systematic evolution of ligands by exponential enrichment) process identify the metal ions using a similar approach of antibodies [12]. Aptamers interact with metal ions by hydrogen bonding, van der Waals forces and hydrophobic accumulation and form particular structures [13]. For examples, the guanine (G)-rich oligonucleotide aptamer utilized for recognition of Pb^{2+} is converted into a G-quadruplex structure in the presence of lead ions [14].

Nanoparticles due to special physicochemical properties can be applied for chemical and biological detection. Among of different nanoparticles used for biosensors, AuNPs have gained increasing attention owing to their high activity and surface-to-volume ratio. These characterizations can supply reactive sites for immobilization of a large amount of biomolecules which are able to retain their bioactivity [15, 16]. For instance, Liu and Lu produced a colorimetric biosensor based on DNAzyme-directed assembly of AuNPs for the detection of lead [17].

In this reserach, an electrochemical aptasensor for Pb^{2+} detection based on the advantages of AuNPs and aptamer have been prepared. For this purpose, a disposable screen-printed carbon electrode was modified with AuNPs and then the Pb^{2+} complementary strand (CS) was immobilized on AuNPs. Next, Pb^{2+} aptamer was added onto the surface of the SPCE to hybridize with CSDNA. After that, the electrochemical cyclic voltammetry experiment was carried out for detection of Pb^{+2} ions. Finally, the properties of the aptasensor including linear range and detection limit were compared with that of other detection methods.

EXPERIMENTAL

Reagents and Materials

The Pb^{+2} aptamer (5'-GGGTGGGTGGGTGG-GT-3') and its complementary strand (5'-Thiol-GAGGACCCACCCACCCACCCTCCTCAA-Thiol-3') were bought from Thermo Fisher Scientific. Hydrogen tetracholoroaurate ($HAuCl_4$), Sodium phosphate dibasic (Na_2HPO_4), potassium phosphate monobasic (KH_2PO_4), potassium chloride (KCl), sodium chloride (NaCl), potassium ferrocyanide ($K_4[Fe(CN)_6]$), potassium ferricyanide ($K_3[Fe(CN)_6]$), Tris(2-carboxyethyl) phosphine hydrochloride (TCEP), 6-mercaptohexanol (MCH) and thionine were purchased from Sigma-Aldrich.

Fabrication process of aptasensor
Preparation of AuNPs-SPCE

The screen printed carbon electrode (SPCE) obtained from DropSens was immersed into a 5 mM $HAuCl_4$ containing 0.1 M H_2SO_4 solution as electrolyte. It should be noted that the SPCE contains a Pt electrode as the auxiliary electrode, an Ag/AgCl electrode as the reference electrode and a carbon electrode as the working electrode. The electrodeposition of gold nanoparticles was done at

a constant potential of -0.4 V versus Ag/AgCl for 60 seconds.

Immobilization of Apt-CS onto AuNPs-SPCE

The CSDNA (10 µL, 2.0 µM) was immobilized onto the surface of AuNPs-SPCE for 60 minutes. Then, 5 µL of 1 mM MCH solution was drop on the surface of the working electrode to block the remaining sites of the SPCE. Next, Pb^{2+} aptamer solution (10 µL, 2.0 µM) was added onto the SPCE surface and incubated for 60 minutes to hybridize with CSDNA.

Preparation of water resuspended AuNPs

AuNPs were firstly synthesized using the classical reduction of $HAuCl_4$ by citrate, based on the previously published procedure [18]. The prepared AuNPs solution was then centrifuged at 15000 g for 30 min at 4 °C.

Characterization of AuNPs-SPCE

The morphological of AuNPs electrodeposited on SPCE, which is obtained from DropSens, was evaluated by a Vega Tescan scanning electron microscope (SEM) equipped with energy dispersive X-ray spectrometer (EDS).

Electrochemical evaluation of developed aptasensor

The interaction of the fabricated aptasensor and lead ions was investigated using cyclic voltammetry (CV) and differential pulse voltammetry (DPV) measurement. All electrochemical experiments were performed in 2 mM $K_4[Fe(CN)_6]$ and $K_3[Fe(CN)_6]$ (redox probe) solution containing 0.1 M KCl using a µStat 400 potentiostat/galvanostat (DropSens, Spain) with three electrode system SPCE. Before measurements, the following treatments were carried out step by step:

The 10 µl of Pb^{2+} (40 nM) was firstly poured on the modified electrode for 60 minutes at room temperature. The modified electrode was then incubated with 10 µl AuNPs (5 nM) for 120 minutes. Next, the 0.5 mM thionine solution was introduced onto the surface of the modified electrode for 15 minutes. After each step of the procedure, the surface of the modified electrode was rinsed with ultrapure water.

Selectivity of the electrochemical aptasensor

The selectivity of the developed aptasensor was investigated in the presence of various cations including Pb^{2+}, Co^{2+}, Zn^{2+}, Cu^{2+} and Ni^{2+}.

RESULTS AND DISCUSSION

SEM analysis of Au-SPCE

The surface morphology of SPCE before and after electrodeposition of AuNPs was illustrated in Fig. 1. As shown in this figure, the micrograph of bare SPCE shows an inhomogeneous and uneven structure. After electrodeposition, it is shown that AuNPs were uniformly distributed on the surface of SPCE (Fig. 1b). Furthermore, EDX analysis of SPCE indicated the presence of electrodeposited gold nanoparticles (Fig. 1c).

Cyclic voltammetry measurements

In this study, CV measurements were performed to evaluate the formation and performance of the prepared aptasensor. As shown in Fig. 2, the bare carbon electrode demonstrated the minimum redox peak current of $Fe[(CN)_6]^{-3/-4}$. After electrodeposition of AuNPs on the surface of SPCE, the peak current significantly increased. It can be related to large surface area to volume ratio of AuNPs which could dramatically intensify the

signals and enhance the electron transfer. The peak current reduced when the complementary strand DNA was adsorbed on the surface of modified electrode. This can be attributed to negatively charged phosphate backbone of the complementary strand, resulting an electrostatic repulsive force to $[Fe(CN)_6]^{3-/4-}$ and prevented the electron transfer [19]. The peak current was further decreased with addition of Pb^{2+} aptamer, demonstrating the hybridization of Apt and CS.

The peak current enhanced by addition of AuNPs, indicating the capture of AuNPs. After addition of thionine, the peak current further increased, illustrating the immobilization of thionine to trapped AuNPs.

It is also shown that peak current increased when the Apt-CS electrode was incubated with Pb^{2+}. It is because that the aptamer releases from complementary strand and form the Apt/target combination. This matter leads to more access of redox species to the electrode surface. Upon addition of thionine-AuNPs, no noticeable change
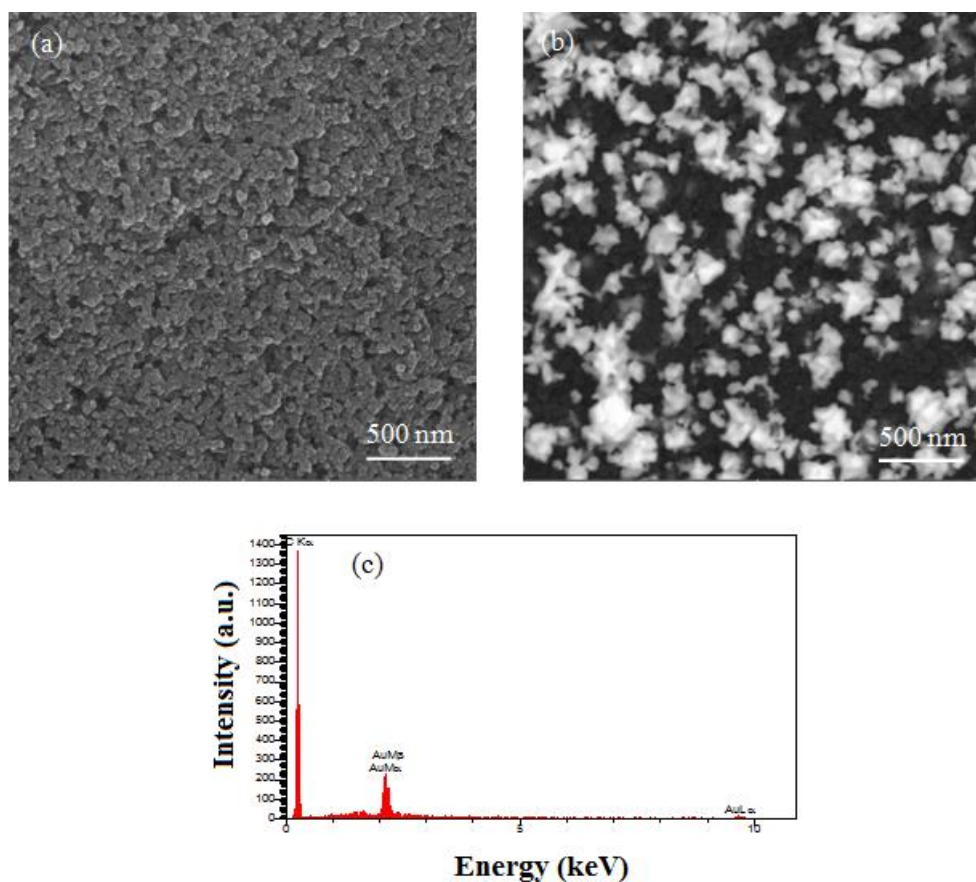

Fig. 1. SEM image of (a) bare SPCE, (b) AuNPs electrodeposited on SPCE and (c) EDS analysis of AuNPs-SPCE.
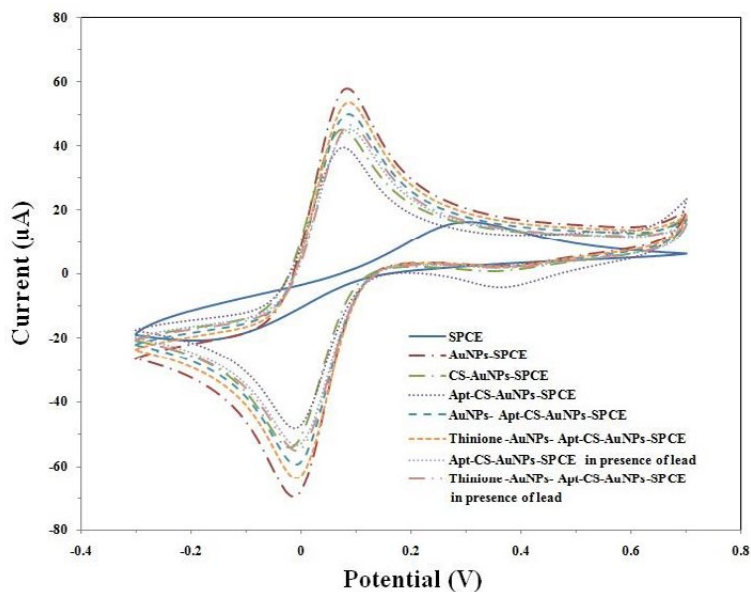
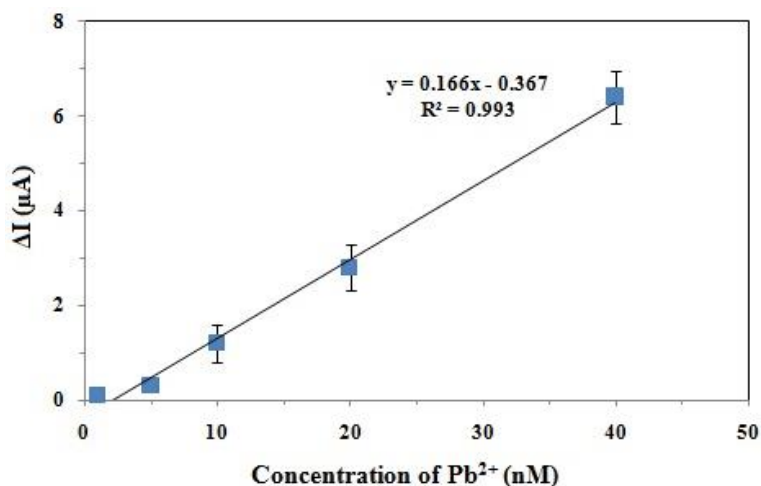Fig. 2. Cyclic voltammetry reponses of different electrodes.

Fig. 3. The linear relationship between DPV peak current changes and Pb^{2+} concentration.

in peak current was observed. It can be due to the formation of hairpin structure of complementary strand and therefore there is no DNA functionalized thionine-AuNPs.

Analytical performance of the aptasensor for Pb^{2+}

The peak current of Apt-CS modified electrode obtained using DPV technique at different concentrations of Pb^{2+} were depicted in Fig. 3. A good linear correlation was illustrated between peak current and the Pb^{2+} concentrations in the range of 1-40 nM. The limit of detection (LOD) was

calculated to be 374 pM based on signal to noise ratio (S/N=3). A comparison of the performance of Pb^{2+} detection in different biosensors is listed in Table 1. It can be observed that the detection limit of Pb^{2+} in this research was relatively better than previous reports.

Selectivity, reproducibility and stability of the developed atpasensor

The selectivity is important factor to evaluate the performance of aptasensor. To investigate the selectivity of aptasensor, the peak current of

Table 1. Comparison between parameters obtained at different biosensors

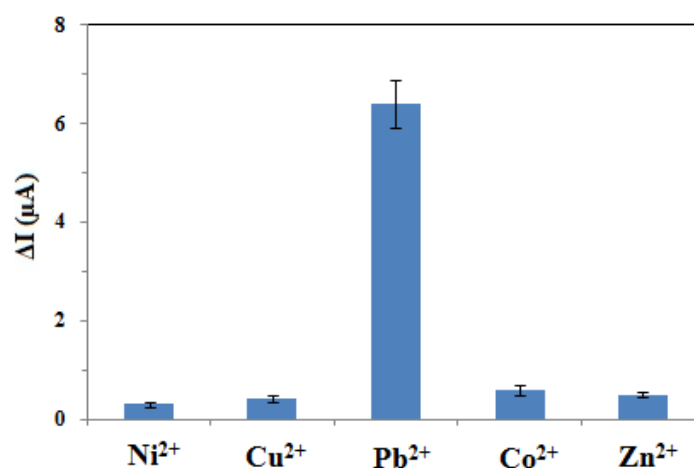| Analytical method	LOD	Linear range	Reference
Colorimetric aptasensor	602 pM	0.2-30 nM	[20]
Electrochemical sensor	0.01 μM	0.05-60 μM	[21]
Electrochemical sensor	0.02 μM	4.8-24.1 nM	[22]
Fluorescence aptamer	60.7 nM	0.009-0.9 nM	[23]
Electrochemical aptasensor	374 pM	1-40 nM	This work

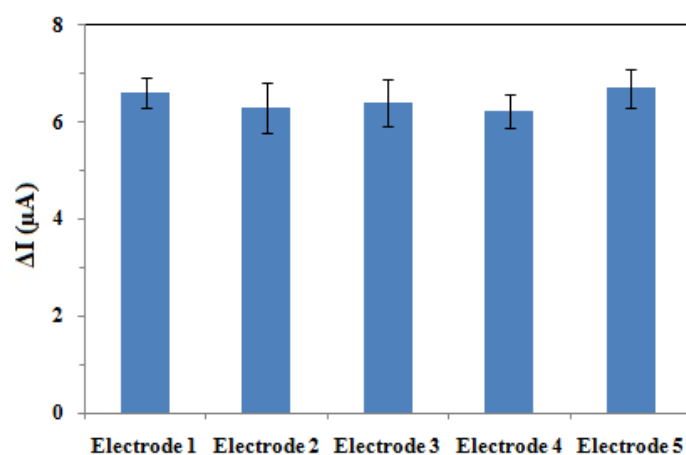Fig. 4. The peak current for different metal ions.

Fig. 5. Peak currents of five electrodes in same conditions.

several common ions was assessed under the same condition. As shown in Fig. 4, no noticeable changes in peak current was observed in the presence of Ni^{2+}, Cu^{2+}, Co^{2+} and Zn^{2+} while the peak current was remarkably increased as Pb^{2+} was added.

The reproducibility of the aptasensor was evaluated using five Apt-CS modified electrodes under the same experimental conditions. The results indicated that aptasensor have a good reproducibility with a relative standard deviation of 2.8% (Fig. 5).

A long-time stability of the aptasensor was investigated for two weeks. After storage the aptasensor in refrigerator (4 °C) for two weeks, the peak current was measured. There was no change significantly in peak current (lower than 5%), indicating that the aptasensor had a long-term stability.

CONCLUSIONS

In this research, a novel electrochemical aptasensor was developed for the selective and sensitive detection of Pb^{2+}. The CV and DPV were performed to investigate the analytical performance of aptasensor. The results exhibited that the aptasensor has a high selectivity, a low detection limit (374 pM), wide linear range (1-40 nM), good reproducibility and long-term stability. Therefore, the aptasensor is promising candidate for the detection of Pb^{2+}.

CONFLICT OF INTEREST

The author declares no conflict of interest.

REFRENCES

1. L. Zhang, G. Zhu, X. Ge, G. Xu, and Y. Guan, *Journal of hazardous materials*, **360**, 32 (2018).
2. H.-B. Wang, L. Wang, K.-J. Huang, S.-P. Xu, H.-Q. Wang, L.-L. Wang, and Y.-M. Liu, *New Journal Of Chemistry*, **37**, 2557 (2013).
3. E. S. Claudio, H. Goldwin, and J. S. Magyar, *Progress in inorganic chemistry*, **51**, 1 (2003).
4. Y.-K. Li, W.-t. Li, X. Liu, T. Yang, M.-L. Chen, and J.-H. Wang, *Talanta*, **203**, 210 (2019).
5. L. Farzin, M. Shamsipur, and S. Sheibani, *Talanta*, **174**, 619 (2017).
6. M. Shahdordizadeh, R. Yazdian-Robati, N. Ansari, M. Ramezani, K. Abnous, and S. M. Taghdisi, *Microchimica Acta*, **185**, 151 (2018).
7. Z. S. Qian, X. Y. Shan, L. J. Chai, J. R. Chen, and H. Feng, *Biosensors and Bioelectronics*, **68**, 225 (2015).
8. J. Ding, D. Zhang, Y. Liu, M. Yu, X. Zhan, D. Zhang, and P. Zhou, *Analytical Methods*, **11**, 4274 (2019).
9. M. Adabi, R. Saber, M. Adabi, and S. Sarkar, *Microchimica Acta*, **172**, 83 (2011).
10. M. Adabi and M. Adabi, *Journal of Dispersion Science and Technology*, 1 (2019).
11. G. Liang, Y. Man, A. Li, X. Jin, X. Liu, and L. Pan, *Microchemical Journal*, **131**, 145 (2017).
12. N. Mor-Vaknin, A. Saha, M. Legendre, C. Carmona-Rivera, M. A. Amin, B. J. Rabquer, M. J. Gonzales-Hernandez, J. Jorns, S. Mohan, and S. Yalavarthi, *Nature communications*, **8**, 14252 (2017).
13. Y. Niu, M. Chu, P. Xu, S. Meng, Q. Zhou, W. Zhao, B. Zhao, and J. Shen, *Biosensors and Bioelectronics*, **101**, 174 (2018).
14. D. Zhang, L. Yin, Z. Meng, A. Yu, L. Guo, and H. Wang, *Analytica chimica acta*, **812**, 161 (2014).
15. Y. Li, H. J. Schluesener, and S. Xu, *Gold Bulletin*, **43**, 29 (2010).
16. S. Guo and E. Wang, *Analytica chimica acta*, **598**, 181 (2007).
17. J. Liu and Y. Lu, *Journal of the American Chemical Society*, **125**, 6642 (2003).
18. J. J. Storhoff, R. Elghanian, R. C. Mucic, C. A. Mirkin, and R. L. Letsinger, *Journal of the American Chemical Society*, **120**, 1959 (1998).
19. F. Zhao, Q. Xie, M. Xu, S. Wang, J. Zhou, and F. Liu, *Biosensors and Bioelectronics*, **66**, 238 (2015).
20. S. M. Taghdisi, N. M. Danesh, P. Lavaee, A. S. Emrani, M. Ramezani, and K. Abnous, *Rsc Advances*, **5**, 43508 (2015).
21. S. Hu, X. Xiong, S. Huang, and X. Lai, *Analytical Sciences*, **32**, 975 (2016).
22. M. Sebastian and B. Mathew, *Journal of materials science*, **53**, 3557 (2018).
23. Y. Chen, H. Li, T. Gao, T. Zhang, L. Xu, B. Wang, J. Wang, and R. Pei, *Sensors and Actuators B: Chemical*, **254**, 214 (2018).